The Astrophysical Journal Letters, 898:L39 (6pp), 2020 August 1 https://doi.org/10.3847/2041-8213/aba42d

Of Harbingers and Higher Modes: Improved Gravitational-wave Early Warning of Compact Binary Mergers

Shasvath J. Kapadia[1], Mukesh Kumar Singh[1], Md Arif Shaikh[1], Deep Chatterjee[2], and Parameswaran Ajith[1,3]
[1] International Centre for Theoretical Sciences, Tata Institute of Fundamental Research, Bangalore 560089, India
[2] Department of Physics, University of Wisconsin–Milwaukee, Milwaukee, WI 53211, USA
[3] Canadian Institute for Advanced Research, CIFAR Azrieli Global Scholar, MaRS Centre, West Tower, 661 University Avenue, Toronto, ON M5G 1M1, Canada
Received 2020 May 21; revised 2020 July 8; accepted 2020 July 9; published 2020 July 29

Abstract

A crucial component to maximizing the science gain from the multi-messenger follow-up of gravitational-wave (GW) signals from compact binary mergers is the prompt discovery of the electromagnetic counterpart. Ideally, the GW detection and localization must be reported early enough to allow for telescopes to slew to the location of the GW event before the onset of the counterpart. However, the time available for early warning is limited by the short duration spent by the dominant ($\ell = m = 2$) mode within the detector's frequency band. Nevertheless, we show that including higher modes—which enter the detector's sensitivity band well before the dominant mode—in GW searches can enable us to significantly improve the early warning ability for compact binaries with asymmetric masses (such as neutron star–black hole (NSBH) binaries). We investigate the reduction in the localization sky-area when the $\ell = m = 3$ and $\ell = m = 4$ modes are included in addition to the dominant mode, considering typical slew-times of electromagnetic telescopes (30–60 s). We find that, in LIGO's projected "O5" ("Voyager") network with five GW detectors, some of the NSBH mergers, located at a distance of 40 Mpc, can be localized to a few hundred sq. deg. ∼45 s prior to the merger, corresponding to a reduction-factor of 3–4 (5–6) in sky-area. For a third-generation network, we get gains of up to 1.5 min in early warning times for a localization area of 100 sq. deg., even when the source is placed at 100 Mpc.

Unified Astronomy Thesaurus concepts: Gravitational wave astronomy (675); Gravitational waves (678); Compact binary stars (283)

1. Introduction

The first gravitational-wave (GW) detection of a binary neutron star (BNS) merger, GW170817 (Abbott et al. 2017a), also produced an electromagnetic (EM) counterpart that was followed up extensively by various telescopes worldwide observing different bands of the EM spectrum (Abbott et al. 2017b). This event became a watershed in multi-messenger astronomy, as it demonstrated the immense science gain in observing the same transient in multiple observational windows. GW170817 verified the previously conjectured engine of short gamma-ray bursts (GRBs) as the merger of BNSs (see Nakar 2007 for a review). In addition, it enabled an unparalleled study of a new class of optical transients called kilonovae (Metzger 2017), which revealed an important environment in which heavy elements get synthesized (Kasen et al. 2017). The multi-messenger observations also provided stringent constraints on the speed of GWs (Abbott et al. 2019a), and gave important clues to the nuclear equation of state (EOS) at high densities (Abbott et al. 2018a, 2019b), and an independent estimation of the Hubble constant (Abbott et al. 2017c).

An early warning of the merger from the GW data would allow many additional science benefits. For example, it would enable the observations of possible precursors (Tsang et al. 2012), a better understanding of the kilonova physics and the formation of heavy elements by identifying the peak of kilonova lightcurves (Cowperthwaite et al. 2017; Drout et al. 2017), and observation of possible signatures of any intermediate merger product (e.g., Hotokezaka et al. 2013) that might have been formed.

BNS mergers are traditionally expected to produce EM counterparts, and therefore it is not surprising that the first efforts toward GW early warning focused on such events. The inspiral of BNSs lasts for several minutes within the frequency band of ground-based GW detectors. If sufficient signal-to-noise ratio (S/N) could be accumulated during this time, ideally tens of seconds to a minute before merger, it could allow for a tight enough sky map for telescopes, enabling them to point at the binary before it merges (Cannon et al. 2012).

Early warning for heavier binaries, like neutron star–black hole (NSBH) binaries or binary black holes (BBHs), is more challenging, given that they spend significantly smaller durations in the band of ground -based detectors (for e.g., GW150914 spent ∼0.1 s in the LIGO detectors' frequency band; Abbott et al. 2016).[4] A possible way to achieve early warning is to detect these systems early in the inspiral, although that would require ground-based detectors to be sensitive at very low frequencies. Seismic noise being the dominant impediment to such low-frequency detections, a "multi-band" detection strategy has been proposed, where the upcoming space-based detector LISA would detect the binary early in its inspiral, potentially years before it reaches the frequency band of ground-based detectors (Sesana 2016).

In this Letter, we describe an alternative method for early warning targeted at unequal-mass compact binaries (especially NSBHs), that could be applied to the upcoming second- and third-generation (2G and 3G) network of ground-based detectors (Punturo et al. 2010; Abbott et al. 2018b; Reitze et al. 2019). The

[4] Stellar mass BBH mergers are not expected to produce EM emissions under standard scenarios. Nevertheless, there are proposals of possible counterparts to such mergers (e.g., Loeb 2016). The Fermi satellite had also announced a candidate gamma-ray counterpart coincident with GW150914 (Connaughton et al. 2016); additionally, the Zwicky Transient Facility recently announced a candidate optical counterpart to a candidate BBH event (Graham et al. 2020).

method essentially relies on the fact that the detected GW signal from asymmetric binary inspirals, within a range of inclination angles, could contain contributions from several higher modes in addition to the dominant, quadrupole ($\ell = m = 2$) mode (e.g., Varma et al. 2014). Since the majority of the higher modes (with $m > 2$) oscillate at larger multiples of the orbital frequency than the dominant mode, we expect these higher modes to enter the frequency band of the detector well before the dominant mode. Thus, using GW templates including higher modes in online GW searches (e.g., Adams et al. 2016; Chu 2017; Messick et al. 2017; Nitz et al. 2018) would enable us to detect and localize the binary earlier than analyses that only use the dominant mode, potentially allowing significant reduction in localization sky-areas, for early-warning times that are comparable to the slew times of a number of EM telescopes (∼30–60 s).

We investigate the reduction in the sky-area (as compared to the same using only the dominant mode) by including the higher modes $\ell = m = 3$ and $\ell = m = 4$ in addition to the dominant mode. We consider binaries with secondary masses spanning the range $m_2 = 1$–$2.5 M_\odot$, mass-ratios $q := m_1/m_2 = 4$–20, located at a GW170817-like distance ($d_L \simeq 40$ Mpc). We find that, for a network of five detectors with projected sensitivities pertaining to the fifth observing run (O5) (KAGRA Collaboration et al. 2019), we get a reduction of sky-area from a few thousand to a few hundred square degrees (a factor of 3–4), for an early warning time of 45 s. These gains increase to factors of 5–6 for the same detector network with the three LIGO detectors, including LIGO-India (Unnikrishnan 2013), upgraded to "Voyager" sensitivity (Adhikari et al. 2019). In a 3G network consisting of two Cosmic Explorers and one Einstein Telescope, for a localization of 100 sq. deg., we can get early-warning-time gains of up to 1.5 min for binaries located at 100 Mpc.

The Letter is organized as follows. Section 2 elaborates on the early-warning method, while also describing higher modes and giving quantitative arguments as to why one should expect them to enhance early-warning times. Section 3 describes the results, in particular the reduction in localization area of the sources by including higher modes and the effect of extrinsic parameters on this reduction, for various upcoming observing scenarios involving ground-based GW detectors. Section 4 gives a summary and an assessment of the benefits of the proposed method.

2. Early Warning with Higher Modes

The gravitational waveform, conveniently expressed as a complex combination $h(t) := h_+(t) - i h_\times(t)$ of two polarizations $h_+(t)$ and $h_\times(t)$, can be expanded in the basis of spin -2 weighted spherical harmonics $Y^{-2}_{\ell m}(\iota, \varphi_o)$ (Newman & Penrose 1966)

$$h(t; \iota, \varphi_o) = \frac{1}{d_L} \sum_{\ell=2}^{\infty} \sum_{m=-\ell}^{\ell} h_{\ell m}(t, \boldsymbol{\lambda})\, Y^{-2}_{\ell m}(\iota, \varphi_o). \quad (1)$$

Here, d_L is the luminosity distance, and $h_{\ell m}$ are the multipoles of the waveform that depend exclusively on the intrinsic parameters of the system $\boldsymbol{\lambda}$ (component masses, spins, etc.) and time t. On the other hand, the dependence of the waveform on the orientation of the source with respect to the line of sight of the detector is captured by the basis functions $Y^{-2}_{\ell m}(\iota, \varphi_o)$ of the spin -2 weighted spherical harmonics, where ι, φ_o are the polar and azimuthal angles in the source-centered frame, that define the line of sight of the observer with respect to the total angular momentum of the binary. For non-precessing binaries, due to symmetry, modes with negative m are related to those with corresponding positive m by $h_{\ell -m} = (-1)^\ell h^*_{\ell m}$. Here we consider only non-precessing binaries. Hence, even when we mention only modes with positive m, it is implied that the corresponding $-m$ modes are also considered.

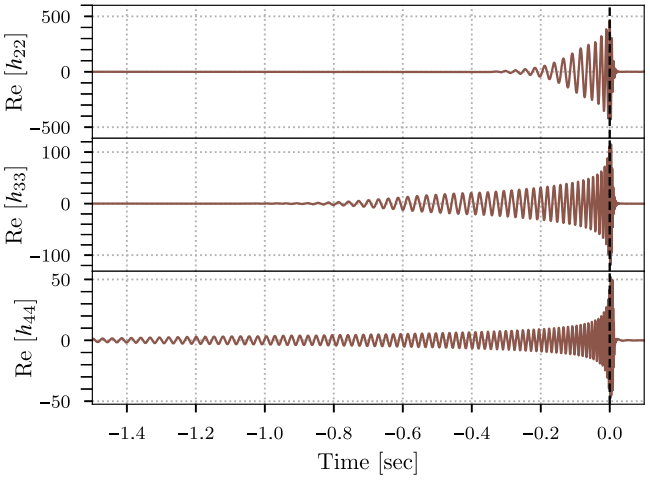

Figure 1. Schematic illustration of how different modes appear in the detector band. We show the real part of the *whitened* modes $h_{\ell m}$ (with $\ell = m = \{2, 3, 4\}$) of a compact binary coalescence waveform ($d_L = 500$ Mpc, $q = 5$, $m_1 + m_2 = 80 M_\odot$), as a function of time. The modes are whitened by the noise power spectral density of Advanced LIGO to show their expected contribution to the S/N. The higher the m, the earlier it enters the frequency band of the detector. This can be seen by the appearance of the non-zero amplitudes of the higher modes at a time $\Delta\tau$ before the merger (dashed black vertical line), where $\Delta\tau$ increases with increasing m.

The dominant multipole corresponds to $\ell = m = 2$, which is the quadrupole mode. The next two subdominant multipoles are $\ell = m = 3$ and $\ell = m = 4$. The contribution of subdominant modes relative to the quadrupole mode depends on the asymmetries of the system—e.g., relative contribution of higher modes is larger for binaries with large mass ratios. Also, due to the nature of the spin -2 weighted spherical harmonics, the higher-mode contribution to the observed signal is the largest for binaries with large inclination angles (say, $\iota = 60°$).

The instantaneous frequency of each spherical harmonic mode is related to the orbital frequency in the following way (assuming a non-precessing orbit):

$$F_{\ell m}(t) \simeq m\, F_{\rm orb}(t). \quad (2)$$

Thus, higher modes (with $m > 2$) enter the frequency band of the detector (say, 10 Hz) before the dominant mode (see Figure 1 for a qualitative illustration).

The time taken by the binary to merge, once it has reached an orbital frequency of $F_{\rm orb}$, is approximately given by (Sathyaprakash 1994)

$$\tau \simeq \frac{5}{256}\, \mathcal{M}^{-5/3}\, (2\pi F_{\rm orb})^{-8/3} \propto (F_{\ell m}/m)^{-8/3}, \quad (3)$$

where $\mathcal{M} := (m_1 m_2)^{3/5}/(m_1 + m_2)^{1/5}$ is the chirp mass of the binary. Thus, the in-band duration of a higher mode $h_{\ell m}$ is a factor $(m/2)^{8/3}$ larger than the corresponding $\ell = m = 2$ mode. For the $\ell = m = 3$ mode, this amounts to a ∼3-fold increase in

the observable duration as compared to the $\ell = m = 2$ mode, and for the $\ell = m = 4$ mode a ∼6-fold increase

However, the time gained in reaching a fiducial threshold S/N or localizing a source to a fiducial sky-area, and the reduction in sky-area at a given early-warning time, depend on two competing factors: on the one hand, higher modes are excited only for binaries with large mass ratios (and hence larger chirp masses, when we fix a lower limit on $m_2 \simeq 1M_\odot$). On the other hand, according to Equation (3), heavier binaries will merge quicker in the detector band. Thus, the region of the m_1-m_2 plane that maximizes the time gains corresponds to regions where the masses are sufficiently asymmetric to excite the higher modes significantly, while not too heavy to make the system hurry through the frequency band of the detector; this region will change depending on the sensitivities of the detectors. Similarly, the reduction in sky-area at a given early-warning time depends additionally on the choice of early-warning time.

For stationary Gaussian noise (which we assume throughout this Letter), the power spectral density (PSD) of the noise completely determines its statistical properties. Based on this assumption, assessing a trigger to be worthy of follow-up can be reduced to setting a threshold on the S/N, corresponding to a given false alarm probability. The localization area, at a given confidence, is determined to a good approximation by the separation of the detectors, their individual effective bandwidths, and the S/Ns. We use the method proposed by Fairhurst (2009, 2011) to estimate the sky area from the times of arrival of the signal at the detectors, and timing uncertainties. In this method, the localization sky area of a source located at a given sky location can be computed from the pair-wise separation of the detectors, as well as each detectors' timing errors. Note that if the detectors are approximately co-planar, then the mirror degeneracy with respect to the plane of the detector needs to be broken by additional waveform consistency tests between detectors.

3. Results

We generate two sets of GW signals: one set containing just the $\ell = m = 2$ mode, while the other includes the $\ell = m = 3$ and $\ell = m = 4$ modes in addition to the dominant mode. These are generated using the IMRPHENOMHM model (London et al. 2018), as implemented in the LALSUITE software package (LIGO Scientific Collaboration 2020). We consider three observing scenarios. The first is the "O5" scenario, consisting of LIGO-Hanford, LIGO-Livingston, Virgo, KAGRA and LIGO-India. We assume the most optimistic projected sensitivities, from the document KAGRA Collaboration et al. (2019). Since KAGRA's projected sensitivity for O5 only has a lower limit, we assume that KAGRA's sensitivity will equal Virgo's. The second is the "Voyager" scenario (noise PSD taken from LIGO Scientific Collaboration 2015), where we assume that all three LIGO detectors, including LIGO-India, will be upgraded to Voyager sensitivity, while Virgo and KAGRA will operate at their O5 sensitivities. The third is the 3G scenario, where the assumed network consists of two Cosmic Explorer detectors and one Einstein Telescope. The projected PSD for the Einstein Telescope is taken from Hild (2012), and that for Cosmic Explorer is taken from Abbott et al. (2017d).

In Figure 2, we summarize the reduction in localization sky-area for a fiducial early-warning time of 45 s, comparable to the slew times of a number of EM telescopes (∼30–60 s), and the early-warning time gained by the inclusion of higher modes for a fiducial sky-area of 1000 sq. deg. We focus on unequal-mass binary systems located at a distance of 40 Mpc (Abbott et al. 2017a), with the secondary mass spanning $m_2 = 1$–$2.5M_\odot$ and the mass ratio spanning $q = 4$–20.[5]

We only show results for the case of non-spinning binaries, since our results do not change appreciably with spin. Furthermore, we focus on the mass range that corresponds to NSBHs. This is done for two reasons: the first is that an EM counterpart for binaries detectable by ground-based detectors are expected to require an NS; the second is that higher modes are excited predominantly for binaries with asymmetric masses ($q \gg 1$). We also include contours that demarcate the region of the m_1-m_2 plane that are expected to produce EM counterparts, based on the spin of the primary and the NS EOS of the secondary (Foucart 2012).[6] For this purpose, we consider three values of the spin (0, 0.6, 0.9), and two EOSs: 2H (Kyutoku et al. 2010) and SLy (Douchin & Haensel 2001). The former is a "stiff" EOS, predicting a relatively broad region of the component-mass space to produce EM counterparts, while the latter is a more "realistic" EOS, as indicated by the GW-based investigations of the properties of GW170817 (Abbott et al. 2019b).

We find that, when higher modes are employed, early-warning sky localization of a few hundred square degrees can be achieved over a significant fraction of the putative "EM-bright" region of the parameter space (Figure 2). This corresponds to a factor of 3–4 (5–6) reduction in sky-area as compared to the same using only the dominant mode in O5 (Voyager). The early-warning-time gains can be as much as ∼25 (40) s in the O5 (Voyager) scenario, for a fiducial sky-area target of 1000 sq. deg. Additionally, Figure 3 summarizes the early-warning-time gains in reaching a localization area of 100 sq. deg., for systems located at 100 Mpc, in the 3G scenario. For binaries that are likely to have EM counterparts even for moderate to low spins of the primary mass, the gains can be as much as a minute.

While Figures 2 and 3 use fixed values of the location and orientation of the binary, Figure 4 shows the variation of the early-warning sky-area as a function of the inclination angle (top plots) and distance (bottom plots), for a binary with $m_1 = 15M_\odot$, $m_2 = 1.5M_\odot$.[7] The sky-area (especially when higher modes are included) is only weakly dependent on the inclination angle, while the improvement over the dominant mode is typically largest for higher inclination angles (where the relative contribution of higher modes is largest). In contrast, sky-area scales as the square of the distance, as expected.

Figure 5 shows the distribution of the early-warning sky-area for the same binary ($m_1 = 15M_\odot$, $m_2 = 1.5M_\odot$) after fixing the inclination to 60° and distance to 40 Mpc, while randomizing over the sky location and polarization angles. For early-warning times of 20, 40, 60 s, the median sky-area after the

[5] We do not consider mass ratios $q > 20$ because the waveforms that we use are calibrated to numerical relativity results only for binaries with $q \lesssim 20$ (London et al. 2018). We also do not show the results for $q < 4$ (and $m_2 > 2.5M_\odot$), as the improvements are not significant.

[6] Note that these regions correspond to the parameter space of binaries that are expected to produce non-zero dynamical ejecta, which is a necessary, but not sufficient, condition for producing EM counterparts.

[7] This choice of masses does not correspond to the optimal mass-combination for time gain, within the mass-space we consider. Nevertheless, it does represent a system that could potentially have an EM counterpart for a moderately $\chi_1 \sim 0.6$ spinning primary assuming a 2H EOS.

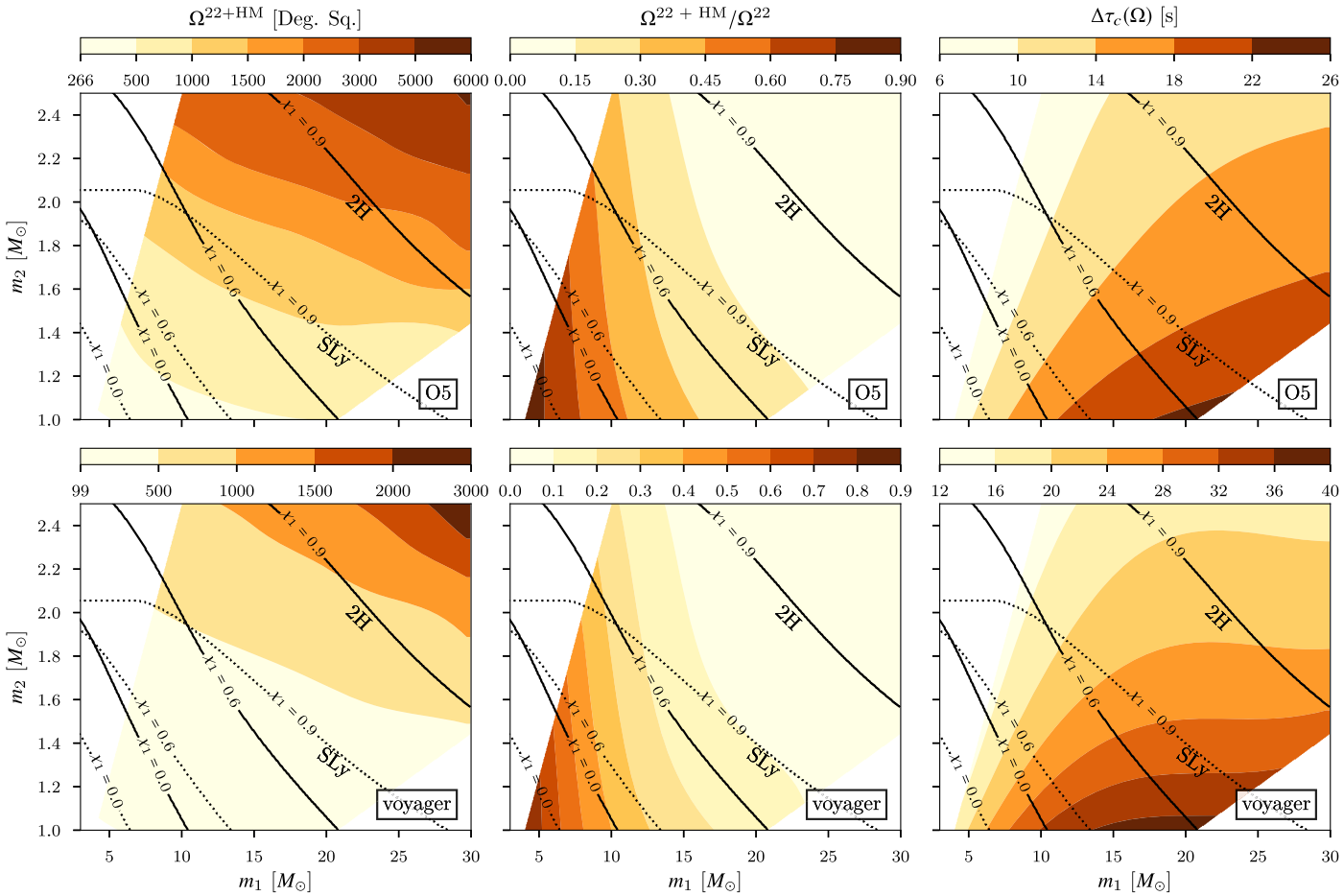

Figure 2. Left plots: localization sky-area (at 90% confidence) using higher modes, for an early warning time of 45 s. Middle plots: the same as a fraction of the sky area achieved using only the dominant modes. Right plots: the gains in the early warning time for a fiducial sky-area of 1000 sq. deg, due to the inclusion of higher modes. These plots correspond to binaries with $m_2 = 1$–$2.5M_\odot$ and $q = 4$–20, located at 40 Mpc (other extrinsic parameters set to their optimal values, with inclination $\iota = 60°$). The compact objects are assumed to be non-spinning; however, even including a primary spin as large as $\chi_1 = 0.9$ does not alter these results significantly. We also plot the contours that demarcate the region corresponding to binaries that would produce a non-zero ejecta mass suggesting the possibility of an EM counterpart, for various χ_1 values (Foucart 2012). Two sets of contours, corresponding to 2H (solid, black contours) and SLy (dotted, black contours) equations of state are plotted. When higher modes are employed, early-warning sky localization of few hundred square degrees can be achieved over significant fraction of the putative "EM-bright" region of the parameter space. This is a factor of 3–4 (5–6) reduction in sky area as compared to the same using only the dominant mode in O5 (Voyager). The early-warning-time gains can be as much as ∼25 (40) s in the O5 (Voyager) scenario.

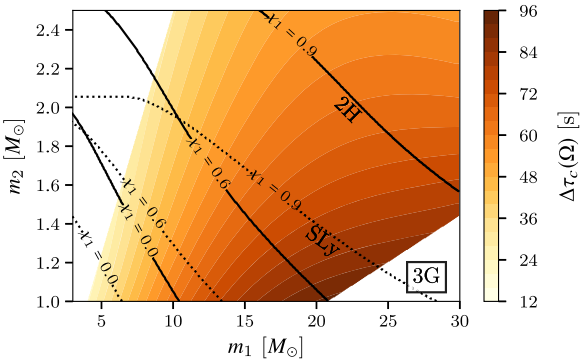

Figure 3. Gains in early-warning time upon inclusion of higher modes, for the 3G scenario, assuming a fiducial sky-area of 100 sq. deg., and sources located at 100 Mpc. The other extrinsic parameters are set to their optimal values, with inclination $\iota = 60°$. These gains can be as much as 1.5 min for relatively low-mass systems that are highly asymmetric. For binaries that are likely to have EM counterparts even for moderate to low spins of the primary mass, the gains can be as much as a minute.

inclusion of the higher modes are 500, 2000, and 8000 (200, 800, and 2000) sq. deg, respectively, for the O5 (Voyager) scenario. We find that for early-warning times of 20 and 40 s, the reduction factor distributions in sky-area are sharply peaked around 28% and 47% (20% and 40%) respectively, for O5 (Voyager). This suggests that the reduction factor is mostly independent of sky location. For a 60 s early warning time, the reduction factor distributions have longer tails, which is a consequence of the fact that for certain sky locations, the sky-area using just the dominant mode saturates to its maximum possible value (∼40,000 sq. deg).

We also estimate the time gained in reaching an S/N threshold of 4 for trigger-selection with the inclusion of higher modes. For O5 (Voyager), we get gains of up to ∼1 (2) min, which correspond to a gain of up to ∼50% (80%), as compared to the same using dominant mode. For 3G, the gains reach 50 min, corresponding to a 500% increase. This could potentially be useful for wide-field telescopes (e.g., all-sky GRB monitors) to discover precursors and prompt emission and to trigger follow-up observations, as we discuss in the next section.

4. Summary and Outlook

Early localization of compact binary mergers from GW data is useful for fast and wide-field surveys (e.g., Bellm et al. 2018; Ivezić et al. 2019) to begin follow-up observations (slew times

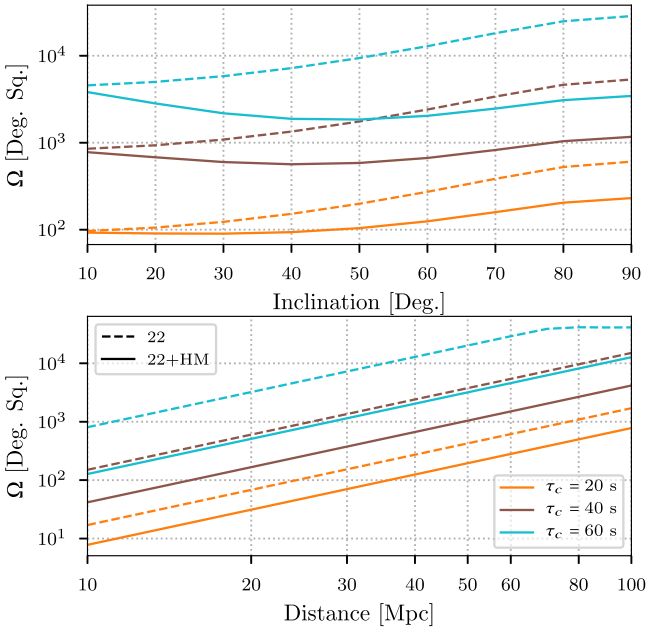

Figure 4. Variation of the sky-area with inclination angle (top panel) and distance (bottom panel) with and without the inclusion of higher modes, for three early-warning times, in the O5 scenario. We pin the masses to $m_1 = 15M_\odot$, $m_2 = 1.5M_\odot$, distance to 40 Mpc, inclination to $\iota = 60°$. (for the bottom panel), and all other extrinsic parameters to their optimal values. The sky-area (especially when higher modes are included) is only weakly dependent on the inclination angle, while the improvement over the dominant mode is typically largest for higher inclination angles (where the relative contribution of higher modes is largest). Sky-area scales as the square of the distance, as expected.

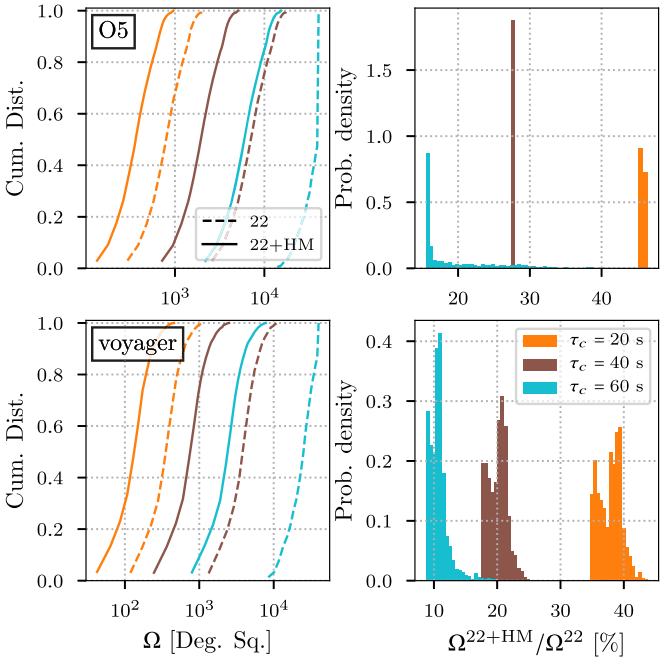

Figure 5. Distributions of the sky-areas for early-warning times of 20, 40, 60 s, with (solid lines) and without (dashed lines) the inclusion of higher modes. The distributions are computed by sampling the parameter space of R.A., decl., and polarization, for a $m_1 = 15M_\odot$, $m_2 = 1.5M_\odot$ system. We set the inclination to $\iota = 60°$, and the distance to 40 Mpc. The rows correspond to different observing scenarios and the columns correspond to (left) sky-area in square degrees and (right) the ratio of the sky-areas with/without higher modes. The median sky-area after the inclusion of the higher modes are 500, 2000, and 8000 (200, 800, and 2000) sq. deg, respectively, for the O5 (Voyager) scenario. These correspond to sky-area ratios of 15%, 28%, and 45% (10%, 20% and 40%) for O5 (Voyager).

∼30–60 s). However, we are limited by the short duration spent by the dominant mode of the gravitational radiation in the detector band. In this Letter, we showed that the inclusion of higher modes in GW low-latency searches will significantly improve the GW early-warning abilities of GW telescopes.[8] This is especially true for asymmetric mass compact binaries with inclined orbits, where higher multipoles of the gravitational radiation are expected to make appreciable contributions to the signal. Recent GW observations have confidently established the existence of some of these higher modes (Abbott et al. 2020a, 2020b).

We find that, using the upcoming five-detector network (O5 or Voyager-type sensitivities) some of the NSBH mergers, located at a distance of 40 Mpc, can be localized to a few hundred square degrees ∼45 s prior to the merger (Figure 2). This corresponds to a factor of 3–4 (5–6) reduction in sky-area in the O5 (Voyager) scenario. For a third-generation network, we get gains of up to 1.5 min in early warning times for a localization area of 100 sq. deg., even when the source is placed at 100 Mpc (Figure 3).

Early-warning localization of a few hundred square degrees is still too large for a single optical telescope to observe in a small number of pointings. However, coordinated observations of several optical telescopes, assisted by a galaxy catalog, can probe the estimated localization region (see, e.g., Coughlin et al. 2018). Additionally, such early warning times could allow telescopes to start slewing toward the general location of the event, thus saving up to around a minute if the telescopes are pointing in very different directions from the source location. With sufficient coordination between the GW network and automated telescopes, it should be possible to track the shrinking localization area, thus optimizing follow-up.

Early warning of a merger might allow wide-field gamma-ray telescopes (with field of view of thousands of square degrees) to trigger on precursors and weak prompt emissions using online sub-threshold analyses, potentially enabling rapid localization of the merger to sub-degree precision (Gehrels 2004).[9] This can facilitate a hierarchy of follow-up observations using X-ray, ultraviolet, and optical telescopes with much smaller fields of view. In the absence of GW early warning, such sub-threshold triggering algorithms might not be used to identify the gamma-ray counterpart, and thus the follow-up observations would not be triggered (Burns et al. 2019).

Advanced early warning with sky-areas spanning thousands of square degrees could be also useful for wide-field radio telescope arrays to dump all the relevant data into storage. These raw data can be analyzed offline to scan the entire localization area to discover any precursors or prompt emission from the merger.

[8] We note that designing sensitive and computationally tractable searches using waveform templates including the effect of higher modes is not a fully solved problem, although efforts in this direction are ongoing (see, e.g., Harry et al. 2018, for some recent work).

[9] Most of the short GRBs are expected to have jet opening angles $\lesssim 20°$ (Berger 2014), for which the expected improvements in the early-warning time due to higher modes are modest (Figure 4). Note, however, that the GRB associated with GW170817 was observed as off-axis, with estimated inclination angle equivalent to $\iota \sim 30°$ (Abbott et al. 2019b).

One might also ask: how often would we expect to see NSBH mergers with counterparts within ∼100 Mpc? Using upper limits on the rate of such mergers from LIGO–Virgo data (Abbott et al. 2019c), as well as from models of formation channels, we could do a more elaborate population study to estimate a distribution of early-warning-time gains. We are currently in the process of producing these results, which we hope to report soon. Even if the rates are not very high, a small number of such golden events might offer some unique glimpses to the complex physics of compact binary mergers.

We are grateful to Shaon Ghosh and the anonymous referee of this article for reviewing our manuscript and providing useful comments. We also thank Stephen Fairhurst for clarifications on Fairhurst (2009, 2011), Srashti Goyal for help with the PYCBC (Nitz et al. 2020) implementation of the antenna pattern functions, and Varun Bhalerao and Shabnam Iyyani for suggestions on possible uses of early warning for gamma-ray and radio telescopes. S.J.K.'s, M.K.S.'s, M.A.S.'s and P.A.'s research was supported by the Department of Atomic Energy, Government of India. In addition, S.J.K.'s research was funded by the Simons Foundation through a Targeted grant to the International Centre for Theoretical Sciences, Tata Institute of Fundamental Research (ICTS-TIFR). P.A.'s research was funded by the Max Planck Society through a Max Planck Partner Group at ICTS-TIFR and by the Canadian Institute for Advanced Research through the CIFAR Azrieli Global Scholars program. DC would like to thank the ICTS-TIFR for their generous hospitality; a part of this work was done during his visit to ICTS.

ORCID iDs

Shasvath J. Kapadia https://orcid.org/0000-0001-5318-1253
Deep Chatterjee https://orcid.org/0000-0003-0038-5468

References

Abbott, B. P., Abbott, R., Abbott, T. D., et al. 2016, PhRvL, 116, 061102
Abbott, B. P., Abbott, R., Abbott, T. D., et al. 2017a, PhRvL, 119, 161101
Abbott, B. P., Abbott, R., Abbott, T. D., et al. 2017b, ApJL, 848, L12
Abbott, B. P., Abbott, R., Abbott, T. D., et al. 2017c, Natur, 551, 85
Abbott, B. P., Abbott, R., Abbott, T. D., et al. 2017d, CQGra, 34, 044001
Abbott, B. P., Abbott, R., Abbott, T. D., et al. 2018a, PhRvL, 121, 161101
Abbott, B. P., Abbott, R., Abbott, T. D., et al. 2018b, LRR, 21, 3
Abbott, B. P., Abbott, R., Abbott, T. D., et al. 2019a, PhRvL, 123, 011102
Abbott, B. P., Abbott, R., Abbott, T. D., et al. 2019b, PhRvX, 9, 011001
Abbott, B. P., Abbott, R., Abbott, T. D., et al. 2019c, PhRvX, 9, 031040
Abbott, R., Abbott, T. D., Abraham, S., et al. 2020a, arXiv:2004.08342
Abbott, R., Abbott, T. D., Abraham, S., et al. 2020b, ApJL, 896, L44
Adams, T., Buskulic, D., Germain, V., et al. 2016, CQGra, 33, 175012
Adhikari, R. X., Ajith, P., Chen, Y., et al. 2019, CQGra, 36, 245010
Bellm, E. C., Kulkarni, S. R., Graham, M. J., et al. 2018, PASP, 131, 018002
Berger, E. 2014, ARA&A, 52, 43
Burns, E., Goldstein, A., Hui, C. M., et al. 2019, ApJ, 871, 90
Cannon, K., Cariou, R., Chapman, A., et al. 2012, ApJ, 748, 136
Chu, Q. 2017, PhD thesis, The Univ. of Western Australia, https://api.research-repository.uwa.edu.au/portalfiles/portal/18509751
Connaughton, V., Burns, E., Goldstein, A., et al. 2016, ApJL, 826, L6
Coughlin, M. W., Tao, D., Chan, M. L., et al. 2018, MNRAS, 478, 692
Cowperthwaite, P. S., Berger, E., Villar, V. A., et al. 2017, ApJL, 848, L17
Douchin, F., & Haensel, P. 2001, A&A, 380, 151
Drout, M. R., Piro, A. L., Shappee, B. J., et al. 2017, Sci, 358, 1570
Fairhurst, S. 2009, NJPh, 11, 123006
Fairhurst, S. 2011, CQGra, 28, 105021
Foucart, F. 2012, PhRvD, 86, 124007
Gehrels, N. 2004, in AIP Conf. Ser. 727, Gamma-Ray Bursts: 30 Years of Discovery, ed. E. Fenimore & M. Galassi (Melville, NY: AIP), 637
Graham, M. J., Ford, K. E. S., McKernan, B., et al. 2020, PhRvL, 124, 251102
Harry, I., Calderón Bustillo, J., & Nitz, A. 2018, PhRvD, 97, 023004
Hild, S. 2012, CQGra, 29, 124006
Hotokezaka, K., Kiuchi, K., Kyutoku, K., et al. 2013, PhRvD, 88, 044026
Ivezić, Ž, Kahn, S. M., Tyson, J. A., et al. 2019, ApJ, 873, 111
KAGRA CollaborationLIGO Scientific CollaborationVirgo Collaboration et al. 2019, Advanced LIGO, Advanced Virgo and KAGRA Observing Run Plans, https://dcc.ligo.org/public/0161/P1900218/002/SummaryForObservers.pdf
Kasen, D., Metzger, B., Barnes, J., Quataert, E., & Ramirez-Ruiz, E. 2017, Natur, 551, 80
Kyutoku, K., Shibata, M., & Taniguchi, K. 2010, PhRvD, 82, 044049
LIGO Scientific Collaboration 2015, Instrument Science White Paper, https://dcc.ligo.org/public/0120/T1500290/002/T1500290.pdf
LIGO Scientific Collaboration 2020, LIGO Algorithm Library—LALSuite, free software (GPL), doi:10.7935/GT1W-FZ16
Loeb, A. 2016, ApJL, 819, L21
London, L., Khan, S., Fauchon-Jones, E., et al. 2018, PhRvL, 120, 161102
Messick, C., Blackburn, K., Brady, P., et al. 2017, PhRvD, 95, 042001
Metzger, B. D. 2017, LRR, 20, 3
Nakar, E. 2007, PhR, 442, 166
Newman, E. T., & Penrose, R. 1966, JMP, 7, 863
Nitz, A., Harry, I., Brown, D., et al. 2020, gwastro/pycbc: PyCBC Release 1.16.4, v1.16.4, Zenodo, doi:10.5281/zenodo.3904502
Nitz, A. H., Dal Canton, T., Davis, D., & Reyes, S. 2018, PhRvD, 98, 024050
Punturo, M., Abernathy, M., Acernese, F., et al. 2010, CQGra, 27, 194002
Reitze, D., Adhikari, R. X., Ballmer, S., et al. 2019, BAAS, 51, 35
Sathyaprakash, B. 1994, PhRvD, 50, 7111
Sesana, A. 2016, PhRvL, 116, 231102
Tsang, D., Read, J. S., Hinderer, T., Piro, A. L., & Bondarescu, R. 2012, PhRvL, 108, 011102
Unnikrishnan, C. S. 2013, IJMPD, 22, 1341010
Varma, V., Ajith, P., Husa, S., et al. 2014, PhRvD, 90, 124004